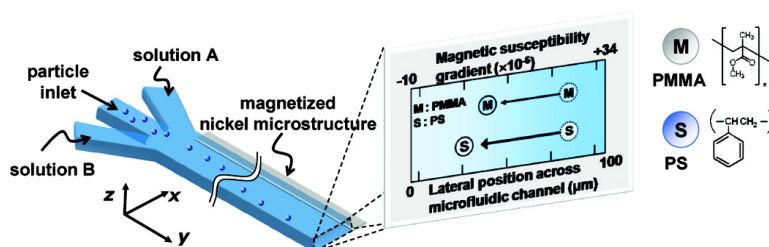


Isomagnetophoresis to Discriminate Subtle Difference in Magnetic Susceptibility

Joo H. Kang, Sungyoung Choi, Wonhye Lee, and Je-Kyun Park

J. Am. Chem. Soc., 2008, 130 (2), 396-397 • DOI: 10.1021/ja0770678

Downloaded from <http://pubs.acs.org> on February 8, 2009



More About This Article

Additional resources and features associated with this article are available within the HTML version:

- Supporting Information
- Links to the 1 articles that cite this article, as of the time of this article download
- Access to high resolution figures
- Links to articles and content related to this article
- Copyright permission to reproduce figures and/or text from this article

[View the Full Text HTML](#)

Isomagnetophoresis to Discriminate Subtle Difference in Magnetic Susceptibility

Joo H. Kang, Sungyoung Choi, Wonhye Lee, and Je-Kyun Park*

Department of Bio and Brain Engineering, Korea Advanced Institute of Science and Technology (KAIST), Daejeon 305-701, Korea

Received September 12, 2007; E-mail: jekyun@kaist.ac.kr

Magnetic susceptibility has been studied diversely in material science,¹ mineralogy,² and biomedical research³ because it is determined by the combination of constituent elements, electrons, chemical bond, and bond–bond interaction⁴ revealing information about molecular property and composition. Determination of magnetic susceptibility in a material is also significant in magnetic resonance (MR) imaging or MR spectroscopy.⁵ Moreover, magnetophoresis based on magnetic susceptibility of materials has been prominent in the demonstration of microparticle analysis,^{6,7} cell separation,⁸ immunoassay,⁹ and single-walled carbon nanotube purification,¹⁰ employing recent microfabrication techniques and a cell tracking velocimetry method. These achievements offered not only the magnetic susceptibility determination but also the continuous separation of the particles having different magnetic susceptibility. However, despite the recent successful applications, a crucial improvement of magnetophoresis should be ahead of further critical application for delicate discrimination and simultaneous separation of various materials.

Here we report an improved magnetophoretic method, isomagnetophoresis, employing the magnetic susceptibility (χ) gradient across a microchannel applied by magnetic field and we have successfully discriminated the polystyrene (PS; $14.78 \pm 0.20 \mu\text{m}$ in diameter), poly(methyl methacrylate) (PMMA; $15.00 \pm 0.77 \mu\text{m}$), and borosilicate (BS; $14.01 \pm 1.00 \mu\text{m}$) microspheres, where PS and PMMA have similar diamagnetic susceptibility⁵ that cannot be distinguished by conventional magnetophoresis. Because the magnetophoretic mobility, m , of a particle is in proportion to $\Delta\chi$ between a particle and surroundings,⁶ it is difficult to discern between the particles having the subtle differences of χ in conventional magnetophoresis. Moreover, m is also directly proportional to the volume of a particle making it hard to be used for discriminating particles with a certain size deviation. Isomagnetophoresis, however, enhances the mobility distinction under the χ gradient of the surroundings, and ideally particles migrate and stay at the net position where the χ of particles and of the surroundings are equal. This principle has an analogy with isoelectric focusing (IEF),¹¹ but the χ gradient is generated by diffusion of two kinds of solution while the pH gradient is created by electrodes aside of the microchannels in IEF. Consequently, the χ profile of the surrounding solution across the microchannel varies as the particles flow along the microchannel owing to the diffusive mass transport. Therefore, we can achieve the ideal isomagnetophoresis if the stationary χ gradient is created over the microfluidic channels employing the hydrogel layer.¹²

The microfluidic device was fabricated by poly(dimethylsiloxane) (PDMS) micromolding processes, and the PDMS channels, slide glasses, and nickel microstructures were assembled by the processes previously reported.¹⁰ The microfluidic device consists of single outlet and three inlets, where the particle-containing

solution flows into the center of the branches and solutions A and B of different χ are injected through the other inlet ports (Figure 1).

While magnetophoresis as a control experiment was carried out using gadolinium paramagnetic diethylenetriamine-pentaacetic acid (Gd-DTPA) solution both for solutions A and B in Figure 1, isomagnetophoresis was demonstrated under the χ gradient using Gd-DTPA (125 mM) and diamagnetic D-glucose (9.3 w/v %) solution (solutions A and B, respectively). For theoretical verification, we established an analytical model composing several functions of magnetic drag velocity, $V_x(t,x)$, χ gradient, $K(t,x)$, magnetic flux density gradient, $B(x)$, and particle velocity driven by the parabolic flow profile, $V_p(x)$ (Supporting Information),

$$V_x(t,x) = - \frac{2R^2(\chi_p - K(t,x))B(x)}{9\mu_0\eta} \quad (1)$$

where $V_x(t,x)$ is the magnetophoretic velocity at time t (s) at position of x , R is the radius of a particle (about $7.5 \mu\text{m}$), χ_p and $K(t,x)$ are the volumetric magnetic susceptibility of a particle and fluid, respectively, $B(x)$ is the magnetic flux density gradient (T^2/m), μ_0 is the vacuum permeability, and η is the dynamic viscosity of fluid. $B(x)$ was estimated by finite element method magnetics (FEMM)¹⁰ and the χ gradient, $K(t,x)$, was calculated by the concentration gradient of each solution in accordance with Wiedemann's additivity law.¹³ The concentration gradient of Gd-DTPA and D-glucose solution was estimated using the finite element method (CFD-ACE+) and an analytical equation, which were confirmed by experimental results (Supporting Information). The lateral positions of the particles were observed by a CCD camera and analyzed by an image-processing program.

In Figure 2a, the lateral positions ($18.52 \pm 1.58 \mu\text{m}$ ($n = 247$) and $18.20 \pm 6.61 \mu\text{m}$ ($n = 802$), respectively, where n is the number of the particles) of PS and PMMA particles are overlapped so that the two types of materials cannot be distinguished. Also a broad deviation of the lateral position (PMMA and BS ($52.13 \pm 5.33 \mu\text{m}$ ($n = 1097$)) results from a large size variation of the particles, and this deviation is proportionate to the size variation as described in eq 1. Isomagnetophoresis, however, in Figure 2b exhibits the pronounced difference of the lateral position of PS ($17.68 \pm 1.62 \mu\text{m}$ ($n = 576$)) and PMMA ($30.44 \pm 3.48 \mu\text{m}$ ($n = 406$)) particles providing the enhanced discernible capability. Furthermore, it remarkably reduces the deviation width of the particle position for all types of particles because the isomagnetophoretic migration is attenuated by the isopoint of χ and the particles stand in the vicinity of the their isopoint without regard for the particle size.

As stated above, the ideal condition for isomagnetophoresis requires the static gradient of χ_{fluid} over the microfluidic channels, but the present device scheme does not provide the stationary χ_{fluid} profiles because of diffusion. Therefore, for theoretical consideration

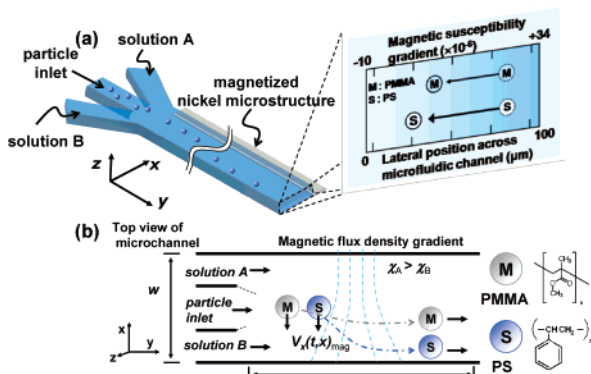


Figure 1. Schematic of isomagnetophoretic discrimination process of particles having subtle difference of magnetic susceptibility (χ_p) in a microfluidic channel.

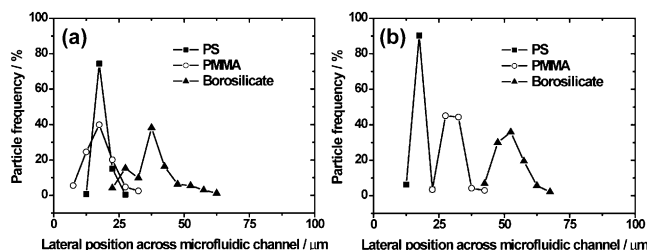


Figure 2. Measured particle position of PS, PMMA, and borosilicate (BS) in conventional magnetophoresis (a) and isomagnetophoresis (b). Subtle difference in magnetic susceptibility between PS and PMMA was preeminently discriminated in isomagnetophoretic displacement (b).

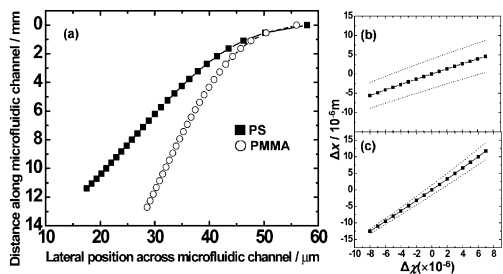


Figure 3. Theoretical estimation of the particle displacement in the microchannels. (a) Particle traces of PS and PMMA particles diverged along the microchannels under isomagnetophoresis. The data points in panel a are the particle position over the microchannel in x - y coordinate system. Magnetophoretic distinction coefficient of isomagnetophoresis (c) is greater than that of conventional magnetophoresis (b). Dashed-lines in panels b and c are expected errors by particle diameter deviation ($\pm 1.0 \mu\text{m}$).

of the present quasi-isomagnetophoretic displacement (due to the transition of the χ_{fluid} gradient in accordance with time and particle position in the y -axis), we employed $V_x(t,x)$ and $V_y(x)$ to estimate the particle displacement at time t . Using this model and the experimental data above, we discriminated χ_{PS} , χ_{PMMA} , and χ_{BS} to be -8.75×10^{-6} , -2.10×10^{-6} , and $+12.90 \times 10^{-6}$, respectively, through isomagnetophoresis, which are comparable with data in the literatures.¹⁴ We were able to compare χ_{PS} because the accurate χ value of various particles has been rarely reported and also because it varies according to the particle density depending on manufacturing processes,⁵ while χ_{PS} has been frequently used in the literature¹⁴ and elsewhere. Figure 3a presents a theoretical prediction of PS and PMMA particles, which reveals a clear correlation of the experimental data as compared to the magnetophoretic prediction (Figure S1b). For the apparent verification of

isomagnetophoresis compared to magnetophoresis, we newly define the (iso)magnetophoretic distinction coefficient in the microfluidic devices, $D = \Delta x / \Delta \chi_{\text{particle}}$, where Δx (10^{-6} m) and $\Delta \chi_{\text{particle}}$ are the difference in the lateral positions of certain kinds of two particles at the outlet (P and Q , $\Delta x = x_p - x_q$) and in magnetic susceptibility ($\Delta \chi_{\text{particle}} = \chi_p - \chi_q$), respectively. We estimated D_{mag} and D_{iso} , considering if the particle P is polystyrene and considering that χ_Q varies from -0.75×10^{-6} to -15.75×10^{-6} . As depicted in Figure 3b,c, isomagnetophoresis provides larger D_{iso} (1.62) compared to D_{mag} (0.67), and moreover, it minimizes the position errors caused by size variations of the particles, supporting the results in Figure 2. The dashed-lines (upper and lower) in Figure 3b,c present data when the particle diameter of P is $15.0 \mu\text{m}$ and the particle diameter of Q is $16.0 \mu\text{m}$ and $14.0 \mu\text{m}$, respectively.

Although isomagnetophoresis demonstrated in this paper is rarely considered to provide tools for single molecular magnetic susceptibility anisotropy, we expect that it can pave the way for the improved magnetic manipulation and sorting of the various materials including cancer cells, nucleic acids, proteins, and carbon nanotubes,^{10,15} discerning the subtle difference in orientation-averaged magnetic susceptibility as we modulate magnetic susceptibility of the injected two solutions and optimize the experimental condition using the analytical model.

Acknowledgment. This work was supported by the Nano/Bio Program (2006-00955, M10503000218-05M0300-21810) of the Ministry of Science and Technology and by the CHUNG Moon Soul Center.

Supporting Information Available: Experimental details, additional data and complete ref 1. This material is available free of charge via the Internet at <http://pubs.acs.org>.

References

- (1) Haddon, R. C.; et al. *Nature* **1991**, *350*, 46–47.
- (2) Bivins, D.; Ergun, S. *Science* **1968**, *159*, 83.
- (3) (a) Wallmann, J. C.; Cunningham, B. B.; Calvin, M. *Science* **1951**, *113*, 55–56. (b) Cerdonio, M.; Congiu-Castellano, A.; Mogno, F.; Pispisa, B.; Romani, G. L.; Vitale, S. *Proc. Natl. Acad. Sci. U.S.A.* **1977**, *74*, 398–400.
- (4) (a) Haberdtz, W. *Angew. Chem., Int. Ed.* **1966**, *5*, 288–298. (b) Gupta, R. R. In *Diamagnetic Susceptibility*; Hellwege, K.-H., Hellwege, A. M., Eds.; Springer-Verlag: Berlin, 1986; Vol. 16, pp 3–10.
- (5) Carlsson, A.; Starck, G.; Ljungberg, M.; Ekholm, S.; Forssell-Aronsson, E. *Magn. Reson. Imaging* **2006**, *24*, 1179–1185.
- (6) Zhang, H.; Moore, L. R.; Zborowski, M.; Williams, P. S.; Margel, S.; Chalmers, J. J. *Analyst* **2005**, *130*, 514–527.
- (7) (a) Fuh, C. B.; Lai, M. H.; Lin, L. Y.; Yeh, S. Y. *Anal. Chem.* **2000**, *72*, 3590–3595. (b) Arase, M.; Suwa, M.; Watarai, H. *Anal. Chem.* **2006**, *78*, 6660–6663.
- (8) (a) Xia, N.; Hunt, T. P.; Mayers, B. T.; Alsberg, E.; Whitesides, G. M.; Westervelt, R. M.; Ingber, D. E. *Biomed. Microdevices* **2006**, *8*, 299–308. (b) Inglis, D. W.; Riehn, R.; Sturm, J. C.; Austin, R. H. *J. Appl. Phys.* **2006**, *99*, 08K101–1–3. (c) Han, K.-H.; Frazier, A. B. *Lab Chip* **2006**, *6*, 265–273.
- (9) (a) Kim, K. S.; Park, J.-K. *Lab Chip* **2005**, *5*, 657–664. (b) Hahn, Y. K.; Jin, Z.; Kang, J. H.; Oh, E.; Han, M. K.; Kim, H. S.; Jang, J. T.; Lee, J. H.; Cheon, J.; Kim, S. H.; Park, H. S.; Park, J. K. *Anal. Chem.* **2007**, *79*, 2214–2220.
- (10) Kang, J. H.; Park, J.-K. *Small* **2007**, *3*, 1784–1791.
- (11) (a) Lu, H.; Gaudet, S.; Schmidt, M. A.; Jensen, K. F. *Anal. Chem.* **2004**, *76*, 5705–5712. (b) Wang, Y.-C.; Choi, M. H.; Han, J. *Anal. Chem.* **2004**, *76*, 4426–4431.
- (12) Wu, H.; Huang, B.; Zare, R. N. *J. Am. Chem. Soc.* **2006**, *128*, 4194–4195.
- (13) Kuchel, P. W.; Chapman, B. E.; Bubba, W. A.; Hansen, P. E.; Durrant, C. J.; Hertzberg, M. P. *Concepts Magn. Reson. Part A* **2003**, *18A*, 56–71.
- (14) Watarai, H.; Namba, M. *Anal. Sci.* **2001**, *17*, 1233–1236.
- (15) (a) Valentine, K. G.; Pometun, M. S.; Kielec, J. M.; Baigelman, R. E.; Staub, J. K.; Owens, K. L.; Wand, A. J. *J. Am. Chem. Soc.* **2006**, *128*, 15930–15931. (b) Volkman, B. F.; Wilkens, S. J.; Lee, A. L.; Xia, B.; Westler, W. M.; Beger, R.; Markley, J. L. *J. Am. Chem. Soc.* **1999**, *121*, 4677–4683. (c) Bryce, D. L.; Boisbouvier, J.; Bax, A. *J. Am. Chem. Soc.* **2004**, *126*, 10820–10821.

JA0770678